Temperature-dependent carrier distributions in $Ga_{1-x}In_xN_yAs_{1-y}$ multiple quantum wells studied by magneto-photoluminescence

T. Nuytten[a)]

Institute for Nanoscale Physics and Chemistry (INPAC), K.U. Leuven, Celestijnenlaan 200D, B-3001 Leuven, Belgium

M. Hayne

Department of Physics, Lancaster University, Lancaster LA1 4YB, United Kingdom

H. Y. Liu[†] and M. Hopkinson

Department of Electronic and Electrical Engineering, University of Sheffield, Mappin Street, Sheffield S1 3JD, United Kingdom

[†]Present address: Department of Electronic and Electrical Engineering, University College London, Torrington Place, London WC1E 7JE, United Kingdom

V. V. Moshchalkov

Institute for Nanoscale Physics and Chemistry (INPAC), K.U. Leuven, Celestijnenlaan 200D, B-3001 Leuven, Belgium

We have investigated the photoluminescence (PL) of two dilute nitride $Ga_{1-x}In_xN_yAs_{1-y}$ multiple quantum well structures in magnetic fields < 50 T. The observation of a nonmonotonic dependence of the PL peak energy on temperature indicates that localised states dominate the luminescence at low temperature, while magneto-PL experiments reveal new insights into the nature of the localisation. We find that the low-temperature spatial distribution of carriers in the quantum well is different for electrons and holes, because they are captured by different disorder-

induced complexes that are spatially separated. A study of the thermalisation of the carriers toward free states leads to the determination of the free-exciton wave-function extent and effective electron mass at low temperatures in these systems. Finally, our experiments enable an assessment of the localisation potentials induced by inhomogeneity in the quantum well, such that an analysis of the PL transition energies at different temperatures results in a phenomenological description of the potential landscape.

I. INTRODUCTION

The incorporation of a few percent of nitrogen in semiconductor quantum wells (QWs) has recently proven to be a valuable approach in reaching long wavelength emission for GaAs-based telecommunication systems.[1-3] In particular, the presence of a small amount of nitrogen in the $In_xGa_{1-x}As$ alloy causes a dramatic red-shift of the host material band-gap and an increased insensitivity of the band-gap energy to temperature, *T*.[4] However, fabrication of high-quality $Ga_{1-x}In_xN_yAs_{1-y}$-based 1.55-μm devices remains a difficult task due to a large miscibility gap, which in turn results in an increased tendency for phase separation and strong carrier localisation.[5,6] Hence, a careful optimization of the growth conditions is required. In the present work we use magneto-photoluminescence (magneto-PL) to study carrier localisation in two contrasting samples: one grown at an elevated temperature and without lattice matching between the QWs and the barrier material, and one with optimised growth temperature and sample morphology. In this way we are able to build up a consistent phenomenological picture of the localisation of electrons and holes in the two samples.

The paper is organised as follows. In Sec. II, we summarise the growth details of the two samples under consideration, describe the experimental setup and introduce the model we have used to analyse the data. Section III discusses the temperature dependence of the PL spectra in the absence of a magnetic field, *B*, as well as the temperature dependent magneto-PL, while the conclusions are summarised in Sec. IV.

II. SAMPLE DETAILS AND EXPERIMENTAL SETUP

The samples in this study, labelled *A* and *B*, were grown on (001) GaAs substrates by molecular beam epitaxy and nitrogen was incorporated using a radio-frequency plasma source.[6,7,8] The active region for sample A was grown at 460°C and consists of a 52 nm $GaN_{0.007}As_{0.993}$ barrier layer followed by five 8 nm $Ga_{0.65}In_{0.35}N_{0.023}As_{0.977}$ QWs between $GaN_{0.007}As_{0.993}$ spacer layers and another $GaN_{0.007}As_{0.993}$ barrier layer. Sample B, grown at 325°C, has the same structure but has three $Ga_{0.62}In_{0.38}N_{0.03}As_{0.97}$ QWs between $Ga_{0.977}In_{0.023}N_{0.01}As_{0.99}$ barriers. The $GaN_{0.007}As_{0.993}$ barriers in sample A are tensile-strained and thus act as strain compensating layers to the compressively strained QWs, while the small addition of indium to the barrier material in sample B reduces the strain at the QW/barrier interface and improves the optical and structural properties of the QW.[6,9] PL spectra were obtained in a He bath and a He flow cryostat at temperatures between 4.2 and 200 K, located in the bore of either a home-made pulsed field coil or a superconducting 12 T magnet. Magnetic field pulses of 20 ms and up to 50 T were delivered using a 5 kV, 500 kJ capacitor bank, during which several PL spectra were recorded using a 30 cm monochromator and a liquid-nitrogen-cooled InGaAs diode array.

The dependence of the centre of mass PL energy, E_{cm}, on magnetic field is analysed using an excitonic model developed by Hayne and co-workers[10] based on a

continuous cross-over between the low-field diamagnetic regime and the high-field Landau-level-like regime. Here, E_{cm} of a complete set of data is fitted using the following equation:

$$E_{cm} = E_0 + \frac{e^2 \left\langle \rho^2 \right\rangle}{8\mu} B^2 \qquad \text{for } B < \frac{2\mathrm{h}}{e\left\langle \rho^2 \right\rangle}$$
$$E_{cm} = E_0 - \frac{\mathrm{h}^2}{2\mu \left\langle \rho^2 \right\rangle} + \frac{e\mathrm{h}}{2\mu} B \qquad \text{for } B > \frac{2\mathrm{h}}{e\left\langle \rho^2 \right\rangle} \tag{1}$$

where e is the charge of the electron, $\hbar$ is the reduced Planck constant and E_0 is E_{cm} at B = 0, allowing the determination of the average exciton wave-function extent, $\left\langle \rho^2 \right\rangle^{1/2}$, and the exciton effective mass μ.

III. RESULTS

In order to investigate the degree of localisation in our samples, we have examined the temperature dependence of the PL energy for both samples (Fig. 1). In agreement with earlier studies,[8,11-14] a nonmonotonic dependence of the PL centre of mass versus T is observed and is attributed to trapping and subsequent detrapping of carriers by localised states. At low T, a slight increase in temperature thermalises the carriers allowing them to reach regions with a higher degree of localisation, recombination from localised states increasingly dominates the PL, and we find a fast red-shift with increasing T, which is due to the temperature-induced trapping of carriers in low energy localised states.

At around 100 K for sample A, and 50 K for sample B, carriers have enough thermal energy to escape the localisation, and redistribution toward the higher energy free-exciton levels occurs, causing a decrease in the population ratio between localised and free excitons. This progressive carrier detrapping from the localised

states shifts the centre of mass of the carrier distribution toward higher energy. Consequently, the PL signal is increasingly dominated by recombination from free excitons, whose energy levels are higher than the localised levels, and a blue-shift is observed. At higher *T*, a band-gap-like red-shift of the PL signal is found, showing that radiation from free excitons only contributes to the PL. Hence, the temperature dependence of the PL energy has a sigmoidal form. The temperature at which the *T*-dependence recovers to a band-gap-like behaviour gives an indication of the degree of localisation, and, in general, an increase in nitrogen content in the QW increases this temperature. Although the nitrogen incorporation in sample B is slightly higher than in sample A (x=0.03 and x=0.023 respectively), the local minimum of the s-shape occurs at higher *T* for sample A and is about 50 % deeper with respect to sample B (Fig. 1), testifying the stronger degree of localisation of the former. Additionally, previous studies have shown that such a small difference in nitrogen incorporation should not have dramatic effects on the properties of the alloy.[6]

The inset to Figure 2 shows the dependence of the PL signal for sample A over six orders of magnitude of laser excitation power density. We observe a clear blue-shift when increasing the excitation power density, a phenomenon that is commonly attributed to spatially indirect recombination.[15-17] However, since we are studying type-I two-dimensional structures, a spatial separation of the charge carriers is only possible by means of localised potential fluctuations that can trap electrons or holes. Indeed, the blue-shift of the PL energy with increasing excitation power has also been attributed to carrier filling of the localised states.[11] The PL peak exhibits a low-energy broadening revealing the presence of localised states, but the signal becomes increasingly more Gaussian at higher excitation powers, indicating that the localised recombination centres tend to saturate at higher excitation power

densities.[18,19] Figure 2 depicts the excitation power density dependence of the PL centre of mass energy over six orders of magnitude. The blue-shift mentioned above is clearly present, and a small kink at powers of about 1 Wcm^{-2} can be noticed. Although it remains unclear what the origin of the change in slope is, we can rule out an excitation-power-induced cross-over to biexcitonic emission: the integrated intensity of the PL signal should have a quadratic dependence on the power density for biexcitons, while a linear scaling is expected for luminescence originating from single electron-hole-pair recombination.[20] As can be seen from Fig. 2, the dependence of the integrated intensity on the excitation power density is entirely linear: no transition to biexcitonic recombination can be distinguished.

PL studies with varying excitation powers for sample B reveal a completely different result. Within the experimental errors, there is no detectable shift of the PL peak for laser power densities increasing over five orders of magnitude (not shown). Since the integrated intensity is, similar to the situation in sample A, characterised by a linear scaling to the excitation power, we conclude that the recombination in sample B is also excitonic, but that the absence of a blue-shift demonstrates a considerable reduction in the localisation of the charge carriers. In order to work out a consistent picture of the exciton localisation in our samples, we have carried out magneto-photoluminescence experiments.

The inset of Figure 3 shows the raw PL spectra for both samples A and B at 0 and 48 T measured at 4.2 K. The low-energy broadening which is a typical manifestation of recombination originating from localised carriers and is commonly observed in $Ga_{1-x}In_xN_yAs_{1-y}$ QWs,[11-13,21,22] is present in the spectra of sample A only, not sample B. Additionally, it can be seen that the line width, measured as the full width at half maximum (FWHM) of the PL signal, is significantly reduced going from

sample A to sample B (from 31 to 22 meV, respectively). The observed inhomogeneous broadening is the result of compositional and structural disorder, which is inevitably present in these quaternary structures,[23] and hence is a reliable parameter to judge the optical quality of our MQW samples. The suppression of the low-energy broadening and the decrease of the line width by about 30 % when going from sample A to sample B confirm that a lower growth temperature and the incorporation of indium in the barrier material (sample B only) have a positive effect on the optical quality of $Ga_{1-x}In_xN_yAs_{1-y}$ MQW structures.[6,9] We should note that apart from a low-energy broadening in sample A, a high-energy feature is present in the PL signal of sample B only. Very little is known up to now about its origin, but we have found that the feature does not exhibit a shift in energy as a function of neither excitation power nor temperature (not shown here), suggesting that it cannot be due to free-exciton recombination. In contrast, we do observe a shift of this feature with magnetic field (inset of Fig. 3), excluding the possibility that it is a trivial artefact related to the experimental setup.

Figure 3 shows the shift of the PL energy, ΔE_{cm}, versus magnetic field for both samples A and B at 4.2 K. The centre of mass of the PL peak of sample B is characterised by a linear dependence on magnetic field right down to the very lowest fields that can be produced with our pulsed fields set-up, whereas the data for sample A show a cross-over from parabolic to linear behaviour at around 8 T, indicating that for sample A, a stronger magnetic field is required to reach the high-field regime. This shows that the exciton wave-functions in sample B, which has indium in the barriers and is grown at lower temperature, are substantially more extended than for sample A at these low temperatures. The spatial extent of the wave

function for an unconfined exciton is related to its effective mass through the Bohr radius

$$a_B = \frac{0.529\varepsilon}{\mu/m_0}\,\text{Å}, \qquad (2)$$

where ε is the dielectric constant and m_0 is the mass of the free electron. Thus, a plausible reason to account for the change in the exciton wave-function we observe is a decrease in μ when going from sample A to sample B. However, an analysis of the data in Fig. 3 gives a very similar effective exciton mass of $(0.090 \pm 0.005)\,\mu_0$ and $(0.0924 \pm 0.0003)\,\mu_0$ for samples A and B, respectively, which is reflected in Fig. 3 by an almost identical slope of the E_{cm} *vs. B* curve in the high-field regime and agrees with previously reported results for dilute nitrides.[24-26] Hence, the change in wave-function extent derived from the difference in magneto-PL at the lowest fields cannot be explained in terms of a change in effective mass. Since the magneto-PL experiments were performed at very low temperatures, we are measuring recombination between electron-hole pairs for which *at least* one carrier is localised. We therefore propose that the reduced wave-function extent measured in sample A is related to the localisation effects already identified in the temperature dependence of E_{cm} (see Fig. 1). At this stage, the data indicate that the localisation keeps the carriers *further apart* for sample B than for sample A.

Although the field dependence of sample B appears linear down to very low fields (see Fig. 3), a small parabolic regime still cannot be completely excluded. Moreover, the longer integration times (> 5 ms) required at higher *T* rule out the pulsed field technique to perform temperature-dependent magneto-PL experiments on our samples. Given the low magnetic fields at which the cross-over between diamagnetic and free-carrier behaviour occurs, magneto-PL in DC fields up to 12 T,

without limitations on the integration time, is an excellent method to study the carrier localisation in more detail, and will help us to distinguish between the effect of localisation on the electrons and the holes.[27] From the pulsed field data we have found that the exciton radius at very low temperatures is substantially more extended for sample B than for sample A since we were unable to detect diamagnetic behaviour for sample B. The analysis of the PL centre of mass energy as a function of DC magnetic field (see inset of Figure 4) reveals a small parabolic regime in fields up to about 4 T at 5 K for sample B. Using Eq. 1 we can then determine an average value for the exciton wave-function extent of 17.5 nm, significantly larger than the corresponding value for sample A, which is 14.5 nm.

The inset to Fig. 4 shows that slightly increasing the temperature from 5 to 50 K moves the cross-over point between the low- and high-field regime for sample B to much higher fields, but that it does not change much going from 50 to 100 K. Correspondingly, the exciton wave-function extent is characterised by a rapid decrease as a function of temperature, followed by an apparent saturation to a value of 12 nm for $T > 50$ K (see Fig. 4), in agreement with earlier studies.[14] For sample A, the situation is similar, but less dramatic. At low temperatures, the excitons are more compact than in sample B (equivalent to what was found in pulsed fields), and a gradual decrease toward the common value of 12 nm at 200 K is observed.

IV. DISCUSSION

In an effort to understand the behaviour we have observed, we will briefly discuss the influence of the growth temperature on the structural and optical quality of $Ga_{1-x}In_xN_yAs_{1-y}$ MQWs as previously studied by various groups.[28-30] Transmission electron microscopy (TEM) studies performed by Herrera *et al.*[29,30] indicate that an

increase in growth temperature enhances In/Ga interdiffusion during growth, which leads to TEM-observable composition fluctuations in the structure. The intensity of the TEM contrast is drastically increased when raising the growth temperature, and for samples grown at very high temperatures (460°C), undulations with a periodicity of 20 nm are observed. The amplitude of the contrast is related to the FWHM of the PL peak in these samples, *i.e.* the TEM-observed degradation of the structural properties when growing at higher temperatures causes a decrease in optical quality. Additionally, the period of the contrasts observed in TEM is reduced when raising the growth temperature, indicating that the scale of the disorder is larger in the samples grown at lower temperatures, although the amplitude is smaller.

This is entirely consistent with our results. Due to the difference in growth temperature also present in our samples, the composition modulation in sample B is reduced with respect to that of sample A, and the length-scale of the disorder in sample B is larger than in sample A. The introduction of indium in the barrier material of sample B reduces the strain at the QW/barrier interface, further lowering the inhomogeneity of the $Ga_{1-x}In_xN_yAs_{1-y}$ QWs in the sample.[6,9] Hence, the effect of carrier localisation is expected to be much stronger in sample A, while the period of the modulation is larger in sample B. The result is that in both samples the electrons may be trapped by nitrogen-rich[26,31] regions, while the holes may only be localised in In-rich parts of the sample, separating them from electrons in the N-rich regions at low temperatures (Fig. 5). In other words, at low *T* the electrons and the holes are being localised at different locations by nitrogen- and indium-rich regions respectively, but the separation is larger in sample B, which was grown under optimised conditions, compared to sample A. Our results clearly corroborate the localisation picture as established by TEM in similar samples:[28-30] the spatial

separation between the electrons and the holes imposed by the disorder-induced local minima in the potential profile is more pronounced in the sample grown at lower *T* due to the increase in the period between composition modulations. In contrast, the activation energy required to free the holes and recover the free-exciton wave-function extent is smaller than in the samples grown at higher *T* due to the shallower localisation potentials: Sample B, which was grown at 325°C, exhibits a larger excitonic wave-function extent (spatial separation of electrons and holes) at low temperatures (~18 nm from the inset to Fig. 4), but this is more rapidly thermally quenched than for the sample A, which was grown at 460°C (separation of ~15 nm).

Between 5 and 50 K, the exciton wave-function extent for sample B drops by about 30 %, while the decrease is only about 7 % for sample A over the same *T* range, indicating that for sample B, the detrapping occurs at lower temperatures, in agreement with the zero-field PL energy dependence on *T* (see Fig. 1). Thermal excitation of the holes from potential fluctuations due to local indium-rich regions into the continuum shifts the nature of the dominant recombination from spatially indirect at low temperature to direct, hence reducing the exciton radius (Fig. 4). At even higher temperatures, the PL signal is dominated by recombination from free excitons, and the exciton wave-function extent saturates. Assuming a simple, thermally-activated exponential decay of the exciton wave-function extent toward the free-exciton radius of 12 nm, we obtain an activation energy of 7.3 meV (84 K) for sample A, while it is only 1.9 meV (22 K) for sample B, and recover the same asymptotic value of 12 nm for the free-exciton extent in both samples (see Fig. 4).

It is interesting to note that the determination of the free-electron wave-function extent enables an assessment of the electron effective mass. At low temperatures, where the electrons are strongly localised, a hole effective mass of

0.09 μ_0 was found for both samples. At high *T*, where neither electrons nor holes are localised, the exciton radius is 12 nm for both samples. Hence, assuming that the introduction of nitrogen has a negligible effect on the dielectric constant of the ternary host material,[32] we can use Eqn. (2) to obtain a value of the electron effective mass of 0.18 m_0. This is similar to what has been reported earlier for nitrogen concentrations below 2 % in GaAsN thin layers,[33] but is larger by about a factor of two than the values reported by the same group for GaInNAs single quantum wells with comparable indium and nitrogen concentrations.[14]

On these grounds and from the observed activation and PL energies, we can then proceed to construct a phenomenological description of the potential landscape in our samples as shown in Figure 5. Zero-field PL energies at low temperatures provide a lower limit for the transitions between potential fluctuations during the initial redistribution toward deeper localisations, while we can estimate the transition energy between electrons localised in nitrogen-rich regions and free holes from the local minima in the sigmoidal *T*-dependence of the PL energy. By extrapolating the band-gap behaviour observed at high *T* toward 0 K, we estimate the band-gap for free excitons, which amounts to 989 and 876 meV for sample A and B, respectively. The energy difference between this extrapolation and the observed recombination energy at the local minimum of the sigmoidal zero-field *T*-dependence of E_{cm} gives a rough estimate of the electron localisation energy in *nitrogen* localisation centres,[34] yielding 21 and 13 meV for sample A and B, respectively. From the exponential modelling of the decrease in exciton radius as a function of *T* we estimate a valence band localisation energy for the *indium* fluctuations of about 7 and 2 meV for samples A and B, respectively. Thus the localisation energies are about twice as large for sample A as for sample B. This is further supported by the behaviour of the data of

Fig. 1, where the temperatures of the maxima and minima also differ by a factor of two for the two samples.

V. CONCLUSIONS

We have investigated the behaviour of the excitonic emission for two $Ga_{1-x}In_xN_yAs_{1-y}$ MQW samples under the application of a strong magnetic field and have proposed a microscopic picture of the localisation effects that are present in these samples. All our observations confirm that the addition of a small percentage (2.3 %) of indium to the barrier material and the lowering of the growth temperature from 460 °C to 325 °C in sample B induce a considerable enhancement of the optical quality of the structure. The nonmonotonic temperature dependence of the PL energy is much weaker and occurs at a lower temperature for the higher quality sample, while magneto-PL experiments evidence an increased electron-hole separation at low temperatures, confirming the existence and nature of composition modulation observed in earlier TEM experiments on similar samples. Thermal quenching of the exciton radius, as observed in the *T*-dependent magneto-PL, is attributed to redistribution of the holes from regions with indium-induced local potential minima into the continuum, allowing them to move to regions where electrons are trapped by an excess of nitrogen. As *T* is further increased, the electrons become free as well, and the PL is dominated by free-carrier recombination. The situation is similar for both samples, but is more dramatic and occurs on a longer length scale for sample B, which was grown at lower temperature and with strain-relieving indium incorporation in the barrier material. An assessment of the potential profiles for both samples from our data leads to the conclusion that the localisation energies are reduced by at least a factor of two in sample B. This assertion is further endorsed by the observation that

for the low quality sample only, an excitation power dependence of the PL signal is found.

We thank Dr. Q. D. Zhuang for useful discussions and comments on the experiments, and M. Capizzi for a critical reading of the manuscript. This work was supported by the Methusalem Funding of the Flemish Government, the Flemish GOA, the Belgian IAP, the Joy Welch Educational Charitable Trust and the EuroMagNET project (contract no. RII3-CT-2004-506239) of the European Commission. M. Hayne acknowledges support of the Research Councils, UK.

[a)]Electronic mail: thomas.nuytten@fys.kuleuven.be

[1]J. S. Harris, Jr., Semicond. Sci. Technol. **17**, 880 (2002).

[2]A. M. Mintairov, K. Sun, J. L. Merz, H. Yuen, S. Bank, M. Wistey, J. S. Harris, G. Peake, A. Egorov, V. Ustinov, R. Kudrawiec, and J. Misiewicz, Semicond. Sci. Technol. **24**, 075013 (2009).

[3]D. Bisping, D. Pucicki, M. Fischer, S. Höfling, and A. Forchel, J. Crys. Growth **311**, 1715 (2009).

[4]E. P. O'Reilly, A. Lindsay, P. J. Klar, A. Polimeni, and M. Capizzi, Semicond. Sci. Technol. **24**, 033001 (2009).

[5]S. R. Bank, H. Bae, L. L. Goddard, H. B. Yuen, M. A. Wistey, R. Kudrawiec, and J. S. Harris Jr., IEEE J. Quantum Electron. **43 (9-10)**, 773 (2007).

[6]H. Y. Liu, M. Hopkinson, P. Navaretti, M. Guitierrez, J. S. Ng, and J. P. R. David, Appl. Phys. Lett. **83**, 4951 (2003).

[7]H. D. Sun, A. H. Clark, H. Y. Liu, M. Hopkinson, S. Calvez, M. D. Dawson, Y. N. Qiu, and J. M. Rorison, Appl. Phys. Lett. **85**, 4013 (2004).

[8]H. Y. Liu, C. M. Tey, C. Y. Jin, S. L. Liew, P. Navaretti, M. Hopkinson, and A. G. Cullis, Appl. Phys. Lett. **88**, 191907 (2006).

[9]H. Y. Liu, W. M. Soong, P. Navaretti, M. Hopkinson, and J. P. R. David, Appl. Phys. Lett. **86**, 062107 (2005).

[10]M. Hayne, J. Maes, S. Bersier, M. Henini, L. Müller-Kirsch, Robert Heitz, D. Bimberg, and V. V. Moshchalkov, Physica B **346-347**, 421 (2004).

[11]A. Polimeni, M. Capizzi, M. Geddo, M. Fisher, M. Reinhardt, and A. Forchel, Phys. Rev. B **63**, 195320 (2001).

[12]A. Polimeni, M. Capizzi, M. Geddo, M. Fisher, M. Reinhardt, and A. Forchel, Appl. Phys. Lett. **77**, 2870 (2000).

[13]L. Grenouillet, C. Bru-Chevallier, G. Guillot, P. Gilet, P. Duvaut, C. Vanuffel, A. Million, and A. Chevenas-Paule, Appl. Phys. Lett. **76**, 2241 (2000).

[14]G. Baldassarri Höger von Högersthal, A. Polimeni, F. Masia, M. Bissiri, M. Capizzi, D. Gollub, M. Fischer, and A. Forchel, Phys. Rev. B **67**, 233304 (2003).

[15]F. Hatami, N. N. Ledentsov, M. Grundmann, J. Bohrer, F. Heinrichsdorff, M. Beer, D. Bimberg, S. S. Ruvimov, P. Werner, U. Gosele, J. Heydenreich, U. Richter, S. V. Ivanov, B. Ya. Meltser, P. S. Kop'ev, and Zh. I. Alferov, Appl. Phys. Lett. **67** 656 (1995).

[16]C. E. Pryor and M. E. Pistol, Phys. Rev. B **72** 205311 (2005).

[17]B. Bansal, S. Godefroo, M. Hayne, G. Medeiros-Ribeiro, and V. V. Moshchalkov, Phys. Rev. B **80**, 205317 (2009).

[18]Y. Sidor, B. Partoens, F. M. Peeters, J. Maes, M. Hayne, D. Fuster, Y. Gonzalez, L. Gonzalez, and V. V. Moshchalkov, Phys. Rev. B **76** 195320 (2007).

[19]F. Ishikawa, A. Guzmán, O. Brandt, A. Trampert, and K. H. Ploog, J. Appl. Phys. **104** 113502 (2008).

[20]K. Matsuda, S. V. Nair, H. E. Ruda, Y. Sugimoto, T. Saiki, and K. Yamaguchi, Appl. Phys. Lett. **90** 013101 (2007).

[21]A. M. Mintairov, T. H. Kosel, J. L. Merz, P. A. Blagnov, A. S. Vlasov, V. M. Ustinov, and R. E. Cook, Phys. Rev. Lett. **87** 277401 (2001).

[22]I. A. Buyanova, W. M. Chen, G. Pozina, J. P. Bergman, B. Monemar, H. P. Xin, and C. W. Tu, Appl. Phys. Lett. **82** 3662 (2003).

[23]E. D. Jones, A. A. Allerman, S. R. Kurtz, N. A. Modine, K. K. Bajaj, S. W. Tozer, and X. Wei, Phys. Rev. B **62** 7144 (2000).

[24]Th. Wimbauer, K. Oettinger, Al. L. Efros, B. K. Meyer, and H. Brugger, Phys. Rev. B **50** 8889 (1994).

[25]I. J. Fritz, T. J. Drummond, G. C. Osbourn, J. E. Schirber, and E. D. Jones, Appl. Phys. Lett. **48** 1678 (1986).

[26]A. Polimeni, F. Masia, G. Baldassarri Höger von Högersthal, and M. Capizzi, J. Phys.: Condens. Matter **16**, S3187 (2004).

[27]M. Hayne, J. Maes, V. V. Moshchalkov, Y. M. Manz, O. G. Schmidt, and K. Eberl, Appl. Phys. Lett. **79**, 45 (2001).

[28]H. Y. Liu, C. M. Tey, C. Y. Jin, S. L. Liew, P. Navaretti, M. Hopkinson, and A. G. Culli, Appl. Phys. Lett. **88**, 191907 (2006).

[29]M. Herrera, D. González, M. Hopkinson, P. Navaretti, M. Gutiérrez, H. Y. Liu, and R. García, Semicond. Sci. Technol. **19**, 813 (2004).

[30]M. Herrera, D. González, M. Hopkinson, M. Gutiérrez, P. Navaretti, H. Y. Liu, and R. García, J. Appl. Phys. **97**, 073705 (2005).

[31]Since the indium- and nitrogen-rich regions across the sample appear in anti-phase [see *e.g.* M. Herrera, D. González, J. G. Lozano, M. Gutierrez, R. García, M. Hopkinson, and H. Y. Liu, Semicond. Sci. Technol. **20**, 1096 (2005)], a lowering of the conduction band due to local indium excess will be compensated by the simultaneous relative absence of nitrogen. The effect of nitrogen incorporation on the conduction band energy is about an order of magnitude stronger than that due to local indium excess, and we can therefore safely consider the nitrogen-rich regions as the dominant localisation centres for electrons.

[32]To our knowledge, only a few groups have reported studies on the effect of nitrogen incorporation on the dielectric constant of III-V compounds, yielding opposite trends with increasing nitrogen concentration. See *e.g.* M. Kondow, M. Uchiyama, M. Morifuji, S. Wu, H. Momose, S. I. Fukushima, A. Fukuyama, and T. Ikari, Appl.

Phys. Express **2** 041003 (2009), A. Gueddim, R. Zerdoum, and N. Bouarissa, Physica B **389** 335 (2007).

[33]F. Masia, G. Pettinari, A. Polimeni, M. Felici, A. Miriametro, M. Capizzi, A. Lindsay, S. B. Healy, E. P. O'Reilly, A. Cristofoli, G. Bais, M. Piccin, S. Rubini, F. Martelli, A. Franciosi, P. J. Klar, K. Volz, and W. Stolz, Phys. Rev. B **73** 073201 (2006).

[34]M.-A. Pinault and E. Tournié, Appl. Phys. Lett. **78** 1562 (2001).

Figure Captions

Figure 1 (colour online): Temperature dependence of the PL centre of mass energy for samples A (triangles) and B (circles). The local minimum in the s-shape, typical for recombination from localised states, is more pronounced and appears at higher *T* for sample A. The data for sample B have been shifted up by 100 meV for clarity.

Figure 2 (colour online): PL centre of mass energy (squares) and integrated intensity (circles) as a function of excitation power density. A clear blue-shift, with a small kink at ~ 1 Wcm^{-2}, is observed, hinting at spatially indirect recombination. The integrated intensity is linearly dependent on the excitation power, confirming that the recombination is excitonic. The excitation power dependence over six orders of magnitude is shown in the inset for sample A. The blue-shift, combined with a reduced importance of the low-energy broadening of the PL peak, is clearly noticeable.

Figure 3 (colour online): The shift of the PL centre of mass energy versus magnetic field. The line is a fit to the data of sample A using Eq. 1. For sample A, a cross-over from parabolic to linear behaviour occurs at 8 T (indicated by the vertical arrow), whereas the data for sample B are linear down to very low fields. The inset shows the PL spectra for both sample A (red) and B (blue) at 0 (full lines) and 48 T (dotted lines) measured at 4.2 K. The low energy broadening is present in the data for sample A only. The line width of the PL peak for sample B is considerably smaller.

Figure 4 (colour online): Exciton wave-function extent as a function of *T* for the DC measurements. At low *T*, the exciton radius in sample B is larger than in sample A,

but as *T* increases, the relation rapidly reverses. Error bars are derived from the uncertainties in the fitting parameters in the analysis of the data following Eq. 1. The PL centre of mass energy shift as a function of DC magnetic field for sample B at 5, 50 and 100 K is shown in the inset. In contrast to the pulsed field data, a small parabolic regime can clearly be observed. The lines are fits to the data using Eq. 1.

Figure 5: Schematic representation of the potential landscape based on our observations. Recombination energies in the figure are derived from PL centre of mass transition energies, and are approximate. The average separation of N-rich and In-rich regions is estimated from our data as being 15 nm for sample A and 18 nm for sample B.

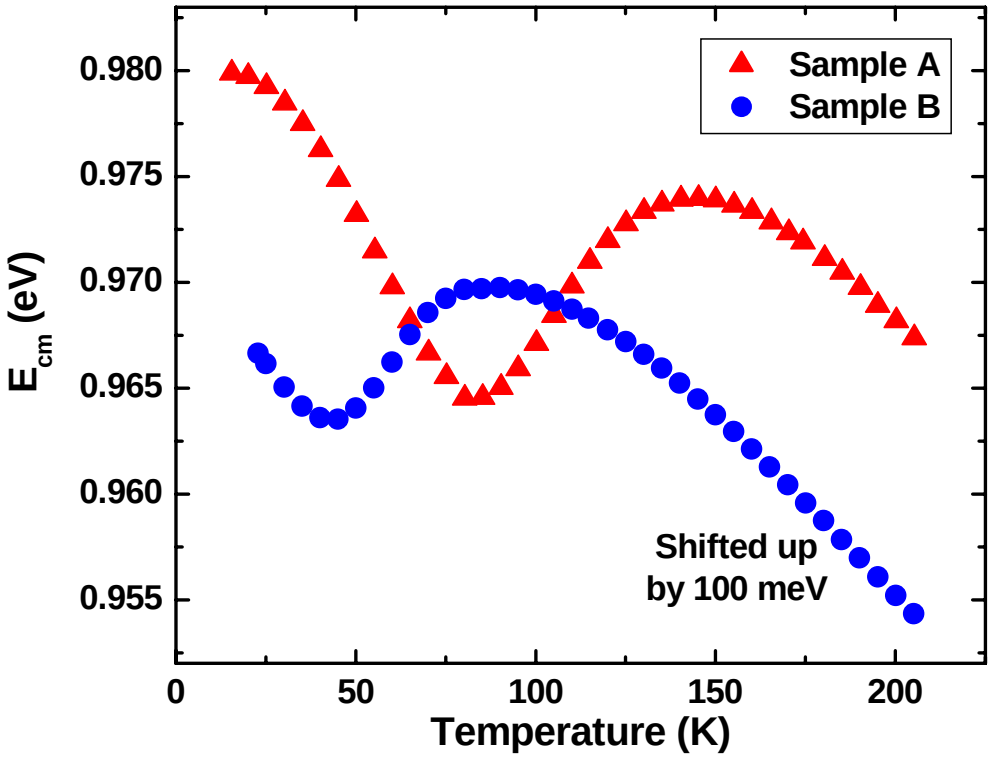

Figure 1 of Nuytten

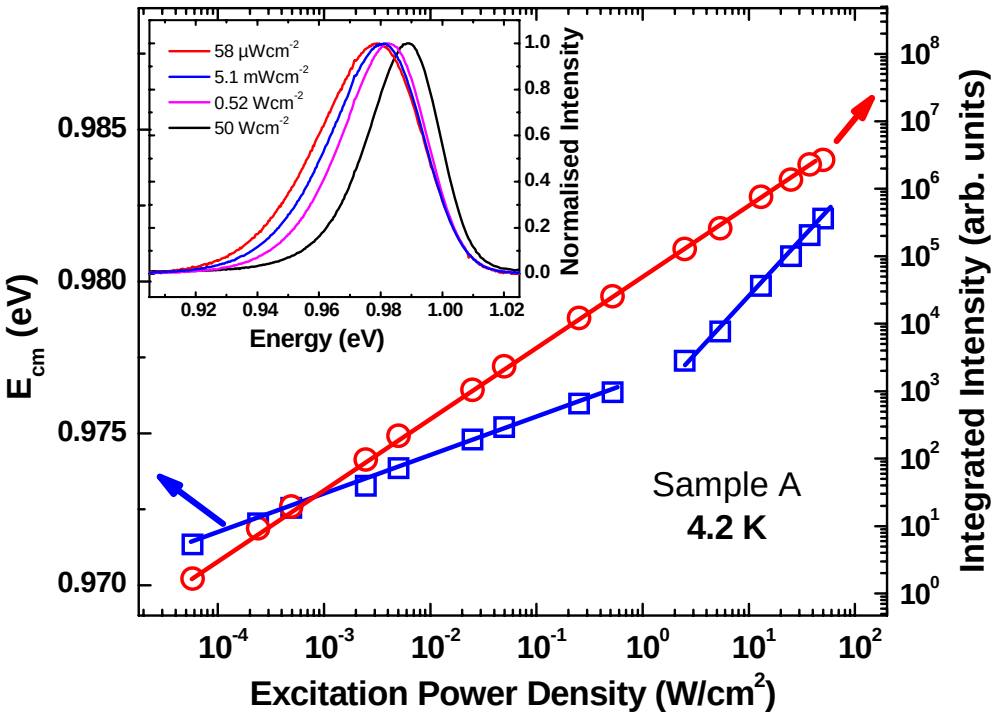

Figure 2 of Nuytten

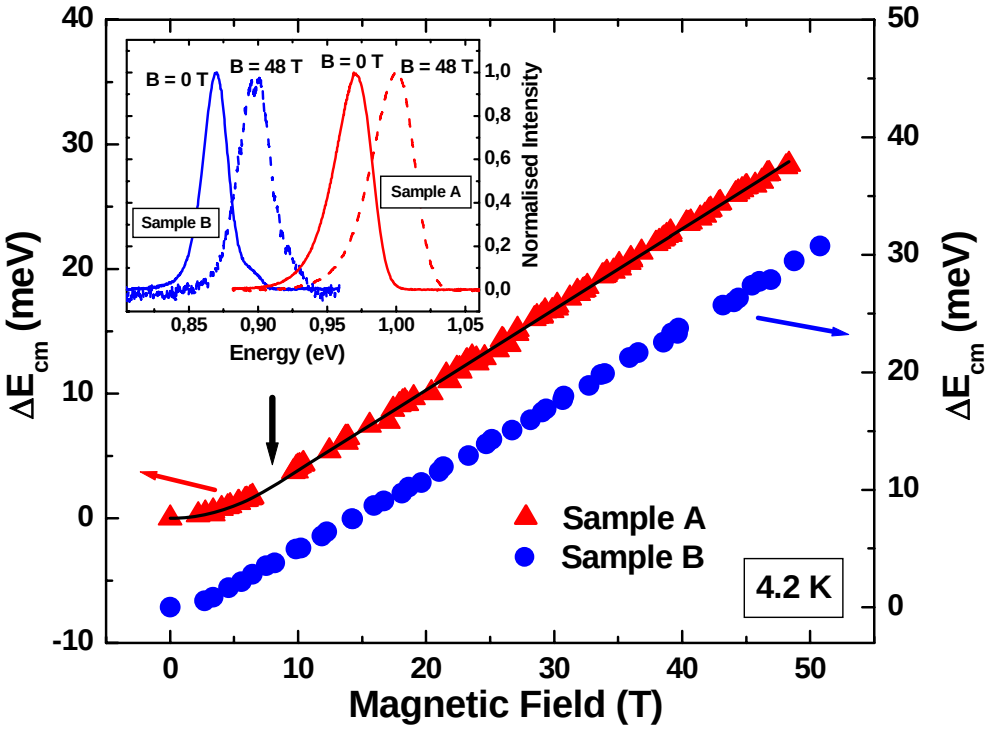

Figure 3 of Nuytten

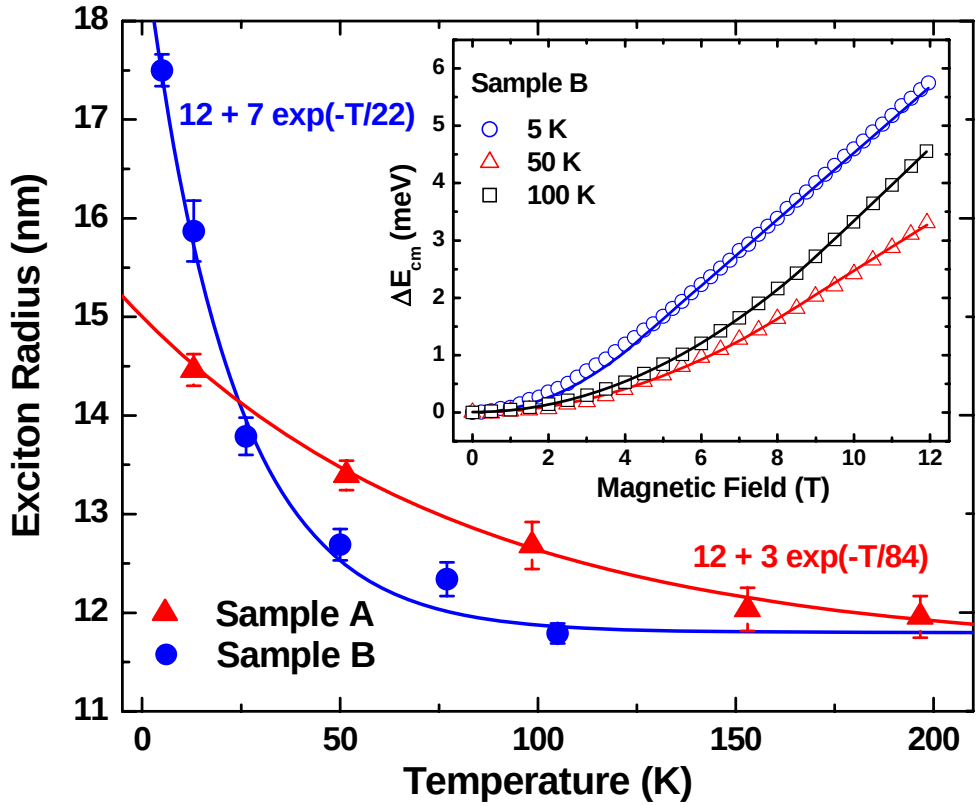

Figure 4 of Nuytten

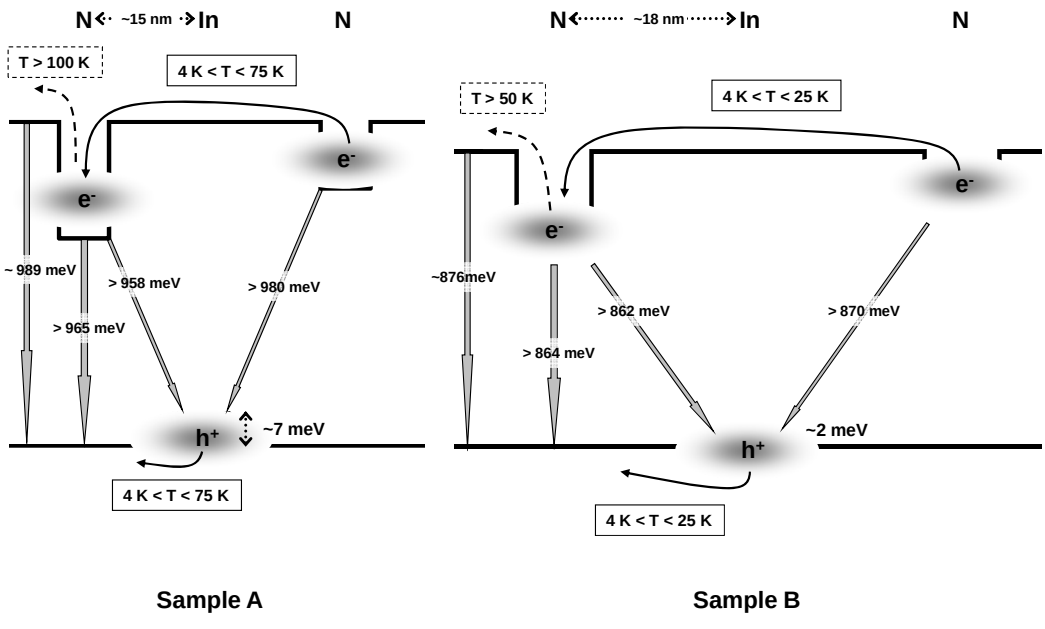

Figure 5 of Nuytten